

Metal Removal Using Fe₃O₄-Chitosan Nanoparticles for Environmental Applications

Remoção de Metais Usando Nanopartículas de Fe₃O₄-Quitossana para Aplicações Ambientais

Emerson Leandro-Silva,^a Maria L. D. C. Silveira,^b Angelo R.F. Pipi,^b Marina Piacenti-Silva,^{a,c} Aroldo G. Magdalena^{b,*} 

^a São Paulo State University, School of Sciences, Graduate Program in Materials Science and Technology, CEP 17033-360, Bauru-SP, Brazil

^b São Paulo State University, School of Sciences, Department of Chemistry, CEP 17033-360, Bauru-SP, Brazil

^c São Paulo State University, School of Engineering, Graduate Program in Civil and Environmental Engineering, CEP 17033-360, Bauru-SP, Brazil

*E-mail: aroldo.magdalena@unesp.br

Recebido: 23 de Setembro de 2022

Aceito: 18 de Setembro de 2023

Publicado online: 10 de Outubro de 2023

Environmental contamination with toxic elements due to increasing anthropogenic activities is of concern because of its direct effects on health and the environment. To help in mitigate this problem, in this study, Fe₃O₄ and Fe₃O₄-chitosan nanoparticles were synthesized, characterized and used as adsorbents to remove metal ions from wastewater samples. The nanoparticles were characterized by X-ray diffraction (XRD), Fourier transform infrared (FTIR) spectroscopy, zeta potential, and transmission electron microscopy (TEM), which confirm that functionalization of the chitosan on the Fe₃O₄ surface was efficient. Inductively coupled plasma atomic emission spectrometry (ICP-AES) analysis determined the metal concentrations in the wastewater samples. The metal adsorption from wastewater showed that Fe₃O₄-chitosan nanoparticles had a removal percentage above 90% for the metals barium, iron, manganese, and zinc. For aluminum, the removal percentage was about 60%.

Keywords: Nanoparticles; chitosan; metal removal; wastewater.

1. Introduction

In 2015 and 2019, Brazil experienced the worst environmental disasters in the cities of Mariana and Brumadinho (state of Minas Gerais), where rivers and tributaries were contaminated with potentially toxic mining residues, including metals.¹ In addition to such disasters, anthropogenic activities can increase metal contamination in the environment, and high concentrations of metals are also found in everyday wastewater, including sewage and industrial wastewater.

Typically, domestic and industrial wastewater are treated by sewage treatment plants (STPs), which are essential in an urbanized society because they improve sanitary conditions and thus promote collective health and sustainability.²⁻⁵ STPs are operational systems that use physical, chemical, and biological processes, to remove pollutants from wastewater and return it to the environment at the appropriate standards for the receiving bodies, in accordance with regulatory requirements.^{6,7}

In many Brazilian cities, wastewater interceptors are installed on the banks of these bodies of water in an attempt to reduce the environmental impact of dumping untreated raw sewage into streams or rivers that flow through the city. However, some of the wastewater in these streams or rivers remains untreated, especially in terms of heavy metal content, which has serious negative effects on human health and the environment. These heavy metals are often higher than the maximum concentrations allowed in Brazil for industrial effluents and/or discharges to receiving waters.^{6,7} This scenario has driven the need to develop techniques and products capable of removing these materials from aqueous media.^{2,3}

Toxic metal removal must consider the preparation of functionalized adsorbents, their affinity, and selective removal. To improve adsorption affinity, a modified surface, including the physical coating and covalent bonds, has often been explored to allow complexation of specific metals. For example, covalent bonds between carboxyl groups and magnetic nanoparticle surfaces were established by the reaction of hematite with 11-undecanoic acid, and the resulting material showed a high capacity for adsorbing Cd(II) ions.⁸ In the literature, Fe₃O₄ nanoparticles coated with chitosan have been reported to be effective in removing Cu(II) ions.⁹ In particular, amino-functionalized materials have shown an excellent ability to remove various heavy metal ions, such as Cu(II), Co(II), Ni(II), Zn(II), Cr(VI), and Cd(II), from aqueous solutions due to the strong capacity for metal complexation with the amino groups.^{3,10}

Several groups have investigated the use of nanomaterials as adsorbents to remove metal ions from wastewater to reduce the environmental impact of high metal concentrations. In principle, some materials, such as magnetic/ferromagnetic nanoparticles, are highly suitable for innovative *in situ* applications because they are versatile tools for adsorbing metals and organic compounds from groundwater, soil and air.⁴ They can be used to remove dyes from residual wastewater from various industries, such as textile mills and tanneries.⁴ Besides, an advantage of these ferrimagnetic nanoparticles is their ability to be functionalized with compounds (chitosan, (3-aminopropyl) trimethoxysilane (APTMS), silica, humic acid) that adsorb metals, thus enhancing the removal of toxic metals from aqueous environments. Other important properties of functionalized magnetic nanoparticles are their large surface area due to their small particle size^{4,10-12} and their intrinsic magnetic field activity, which increases the ability and efficiency of separating different metal ions and facilitates metal removal from aqueous media after adsorption.¹³

Our research group has studied aspects of metal removal and the influence of physical and chemical parameters of two wastewater outfalls on the Bauru River, where the concentrations of elements such as Al, Cu, and Fe were above the legal reference limit.^{14,15} Concerned about the high levels of metals found, our group has been working on the development of adsorbents for metal removal. Thus, the aim of this study is to present the synthesis and characterization studies of Fe₃O₄-chitosan nanoparticles and to evaluate their performance in removing metals from wastewater samples collected from the two sewage outfalls of the Bauru River in Bauru, São Paulo, Brazil.

2. Materials and Methods

2.1. Nanoparticle synthesis

All chemicals were of analytical grade, and all solutions were prepared with ultrapure water. The materials used in this study were FeCl₂·4H₂O (Synth), FeCl₃·6H₂O (Aldrich), ammonium hydroxide (NH₄OH) (Synth), low molecular weight chitosan (75-85% deacetylated/Aldrich), sodium hydroxide (NaOH) (Dinâmica), acetic acid (Synth), and nitric acid (Synth).

Fe₃O₄ nanoparticles were synthesized by the co-precipitation method.¹⁶⁻²² For this synthesis, 0.05 mol L⁻¹ of FeCl₃·6H₂O and 0.025 mol L⁻¹ of FeCl₂·4H₂O were prepared. The precursors were mixed in 300 mL of distilled water and kept at room temperature with continuous stirring under a bubbling inert N₂ atmosphere to remove excess oxygen from the solution. After 10 minutes, NH₄OH was added dropwise until a pH of 9.5 was reached, as evidenced by a black precipitate. The system was mechanically stirred at *ca.* 200 rpm for one hour under a bubbling inert N₂ atmosphere to prevent oxidation of magnetite (Fe₃O₄)

nanoparticle into maghemite (γ-Fe₂O₃) and hematite (α-Fe₂O₃).^{16,21} Next, the nanoparticles were magnetically separated and washed with water until a neutral pH was reached. The nanoparticles were then dried in a rotary evaporator system at 60 °C.

For Fe₃O₄-chitosan functionalization, a solution of 1000 mg of chitosan was prepared in 300 mL of a 2% acetic acid solution. To this solution, 1000 mg of Fe₃O₄ nanoparticles were dispersed and stirred for one hour. Later, 50 mL of a 5 mol L⁻¹ NaOH solution was added dropwise to encapsulate the nanoparticles with chitosan.²²⁻²³ The washing and drying procedures were identical to those performed for Fe₃O₄ nanoparticles.

2.2. Characterization techniques

Nanoparticle samples were characterized by transmission electron microscopy (TEM) using a Philips CM-200 instrument. The Fe₃O₄ and Fe₃O₄-chitosan were dispersed in isopropyl alcohol and kept in an ultrasonic bath. A few drops of the system were placed on the copper grid covered with carbon film. X-ray diffraction was performed with a Rigaku-Rint 2000 diffractometer using CuKα radiation with λ = 1.5418 Angstrom. Measurements were performed at the 2θ interval between 10 and 80° at a scanning speed of 0.04° min⁻¹. Experimental Zeta potential data were collected in the Zetasizer Nano ZS System, Malvern Instruments. During data collection, the pH variation was controlled using 0.1 mol L⁻¹ HCl and NaOH in 0.001 mol L⁻¹ NaCl with supporting electrolyte. The mid-infrared spectra were obtained with a Vertex 70 spectrometer (Bruker Instruments) using the attenuated total reflectance (ATR) method and a scanning range of 4000-400 cm⁻¹ with diamond crystals. Inductively coupled plasma atomic emission spectrometry (ICP-AES) was performed using the Optima 8000 model (Perkin-Elmer). Particle size was calculated by image analysis using the free software Image J.

2.3. Sample collection and preparation

Samples were collected and prepared according to standard methods for the investigation of water and wastewater.²⁴ Wastewater samples were collected at a raw wastewater treatment plant prior to discharge into the Bauru River at Nuno de Assis Avenue (22° 19' 09.6" S and 49° 04' 34.2" W) in Bauru, São Paulo, Brazil. Samples were collected during the second half of 2019. According to the city administration, the samples were composed of domestic wastewater only.

A stainless steel collector was used for sampling. The collector was previously cleaned and rinsed with the sample prior to final collection. Next, 2.0 L of the sample was transferred to high-density polyethylene (HDPE) bottles and identified. The average pH for all samples was about 7. Immediately after collection, the samples were sent to the laboratory, where they were acidified to pH < 2 by adding

nitric acid and kept refrigerated at 4 °C until digestion and/or adsorption procedures.

Part of the wastewater samples were digested prior to adsorption in order to evaluate the total metal content. Thus, 45 mL of the samples were digested with 5 mL of ultrapure nitric acid in a microwave oven (Ethos Easy model) to degrade the organic matter according to the standard methods for the analysis of water and wastewater.²⁴ Digestion was programmed for 10 minutes from 25 to 160 °C, 40 minutes from 160 to 170 °C, and further cooling to reach room temperature (25 °C).²⁵ The other part of the samples was digested after adsorption to evaluate the residual metal content. All procedures were performed in triplicate.

Prior to analysis of the wastewater samples, the ICP-AES metal quantification method was validated using a reference material from the Environment and Climate Change Canada Proficiency Testing Studies (A2LA accredited), an environmental matrix reference material (TMDA 62.2, lot 0618). The reference sample was subjected to the aforementioned digestion process to evaluate the application of the digestion method. After quantitative analyses, all samples were multiplied by 1.10 to correct for metal concentrations by adding 5 mL of nitric acid (10%).

2.4. Evaluation of metal removal

Quantitative analyses of metals before and after adsorption were performed using ICP-AES. The following metals were evaluated: Al(III), Ba(II), Pb(II), Cu(II), Cr(III), Fe(II), Mn(II) and Zn(II). For the adsorption test, the contact time was fixed at 60 minutes at room temperature of 26 °C (±2), pH value of 7 (the same as samples in nature), continuous mixing throughout the process, averaging 300 rpm, with a mechanical stirrer.²² These parameters of adsorption were previously established as the best ones for this adsorbent.^{21,22}

The percentage of metal removal was evaluated using the batch method. The adsorption procedure started from the wastewater sample solutions before digestion. Adsorbent mass (100.0 mg) and adsorbate volume (25.00 mL) were set for all experiments. Removal percentage (%) was calculated using equation (1).^{22,26-27}

$$\% = \left(\frac{C_o - C_e}{C_o} \right) 100 \quad (1)$$

where C_o and C_e are initial and final concentrations, in mg L⁻¹, respectively.^{22,26-27}

3. Results and Discussion

Figure 1 shows the X-ray diffraction (XRD) results for Fe₃O₄-chitosan samples. The crystallographic planes in the pattern showed in Figure 1 refer to magnetite (JCPDS card

n. 89-0688). This result indicates that modification of the magnetite surfaces with chitosan does not change or create different crystallographic planes. The small shoulder at the baseline around $2\theta = 20^\circ$ corresponds to the contribution of chitosan in the Fe₃O₄-chitosan nanoparticles.²³ For the most intense diffraction peak shown in the XRD pattern of Figure 1, an estimation of the particle size was obtained using the Scherrer equation.^{21,28} The value found was 19.9 nm, which is consistent with the size of Fe₃O₄ nanoparticles using co-precipitation as the synthesis method.^{21,29}

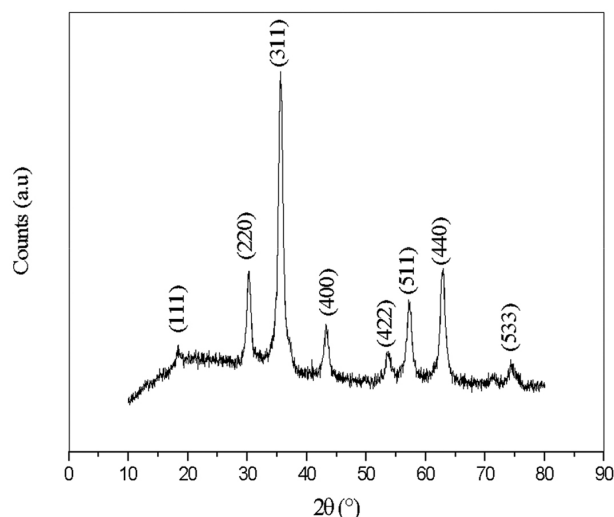


Figure 1. X-ray diffraction pattern of Fe₃O₄-chitosan nanoparticles

Figure 2 shows the results of FTIR spectra for Fe₃O₄ and Fe₃O₄-chitosan nanoparticles.

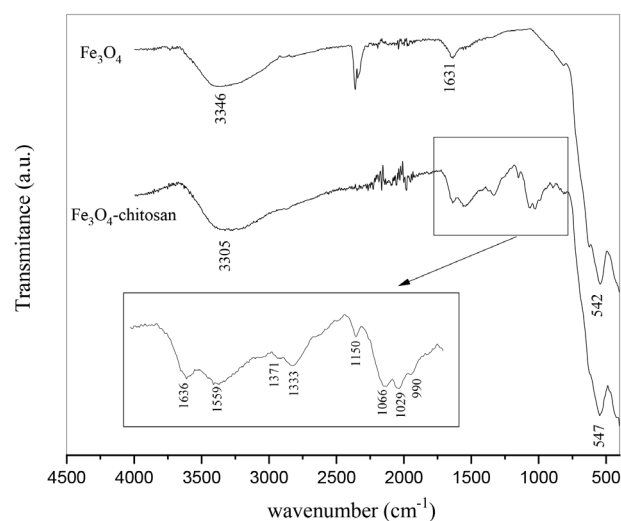


Figure 2. Infrared spectra of Fe₃O₄ and Fe₃O₄-chitosan nanoparticles. The main bands are shown in the inset

The FTIR spectrum for the Fe₃O₄ nanoparticles shows three main bands. The first one is at around 542 cm⁻¹ and is related to Fe-O bonds and indicates the Fe₃O₄ formation. The bands around 1631 and 3346 cm⁻¹ are related to the adsorption of water molecules.^{17,21}

In previous work of our group,²³ the IR spectrum of pure chitosan was obtained. The main bands were: 3315, 1654-1654, 1580-1559, 1420, 1370, 1317-1259 and 1190-890 cm^{-1} . The band at 3315 cm^{-1} corresponds to the stretching of the (-OH) group and with the stretching of the N-H bond. The interval 1654-1654 cm^{-1} is due to the presence of adsorbed water molecules and axial deformation of amide C=O also occurs. The interval 1580-1559 cm^{-1} is associated with the angular deformation of N-H. The band at 1420 cm^{-1} is associated with the axial deformation of the -CN amide. The symmetrical angular deformation of CH_3 and the deformation of the primary alcohol are occurring in 1370 cm^{-1} . In the interval of 1317-1259 cm^{-1} is associated with the -CN deformation of amino groups. The polysaccharide structures of chitosan correspond to the bands in the interval of the 1190-890 cm^{-1} .^{23,30,31}

The functionalization of Fe_3O_4 nanoparticle surfaces with chitosan (Figure 2) was efficient and confirmed by the appearance of new bands related to chitosan.^{23,30,31} The band associated with the Fe-O bond vibration shifted to 547 cm^{-1} in Fe_3O_4 -chitosan nanoparticles. According to Bini *et al.*,¹⁷ the Fe-O bond vibration shifts to higher wavenumbers when a chemical bond is formed between the surfaces of magnetite nanoparticle and other compounds. The absorption of water molecules was associated with the band at 1636 cm^{-1} , and the angular deformations of N-H and CH_3 were associated with bands at 1549, 1333, and 1371 cm^{-1} . The deformation of the primary alcohol bond of chitosan should occur in the interval of 1371 cm^{-1} , together with the angular deformation of CH_3 . In addition, the axial deformation of -CN from amino groups may be associated with the 1330 cm^{-1} band, and the 1150-990 cm^{-1} intervals

were attributed to polysaccharide structures of chitosan.³⁰⁻³¹ The band at 3305 cm^{-1} is associated with $\nu(\text{O-H})$ and N-H stretching.¹⁸ These results confirm the functionalization and formation of Fe_3O_4 -chitosan nanoparticles.

Figures 3(a) and 3(b) show TEM images for Fe_3O_4 and Fe_3O_4 -chitosan nanoparticles, respectively. The TEM in Figure 3(b) indicates that chitosan coats the clusters of Fe_3O_4 nanoparticles, and the histogram in Figures 3(c) and 3(d) shows a Fe_3O_4 and Fe_3O_4 -chitosan nanoparticle size of 15 ± 5 nm and 17 ± 7 nm, respectively.

Figure 4 shows the analysis of nanoparticle surfaces from zeta potential measurements. The zero-point charge (ZPC) depends on several synthesis conditions. Magdalena *et al.*²¹ found a PZC value around 6 for Fe_3O_4 nanoparticles under the same conditions (synthesis temperature (25 °C) and atmosphere (N_2)). Zhao *et al.*³⁰ and Vieira *et al.*³¹ found PZC values in the intervals 6 and 6-10, respectively. The same 6-10 interval was found for natural and cross-linked chitosan membranes.²⁹ The estimated PZC from the zeta potential curve in Figure 4 was 9.2. Our results show that magnetite functionalization shifted the zero-point charge to higher pH values, from 6.0 for Fe_3O_4 ²¹ to 9.0 for Fe_3O_4 -chitosan nanoparticles. This value is in agreement with Vieira *et al.*³¹ and confirms that chitosan modified the Fe_3O_4 nanoparticle surfaces. Moreover, at pH levels below 6.0, Fe_3O_4 -chitosan nanoparticles exhibited higher colloidal stability than Fe_3O_4 nanoparticles.²¹

These XRD, TEM, FTIR, and zeta potential results confirm that chitosan chemically modified Fe_3O_4 nanoparticles. Leandro-Silva *et al.*²² investigated the adsorptive efficiency of Fe_3O_4 -chitosan nanoparticles and a bioadsorbent based on banana peel flour against a synthetic

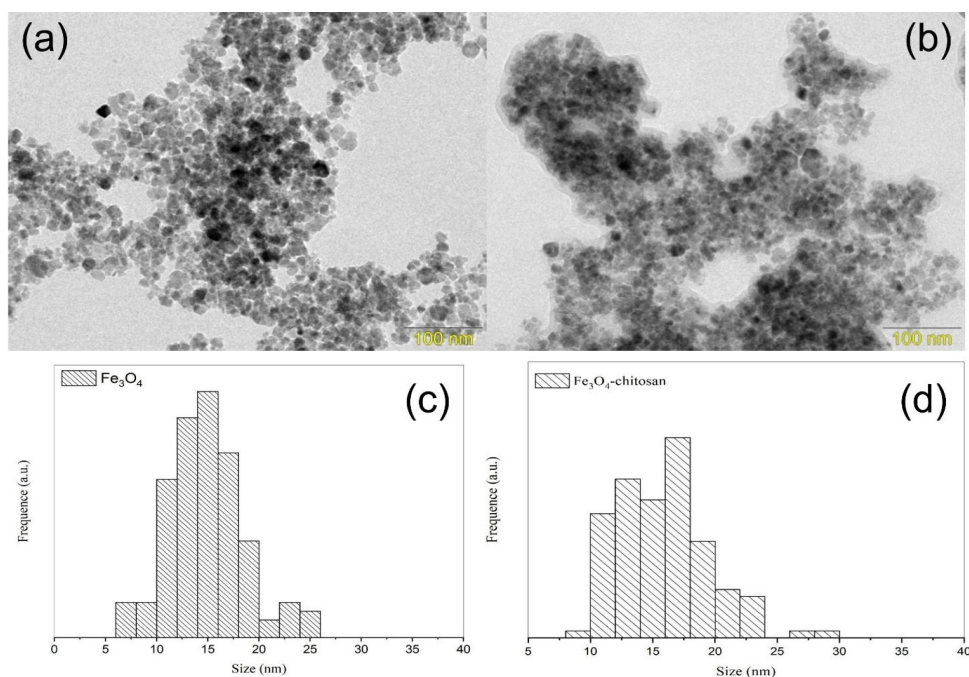


Figure 3. TEM images of (a) Fe_3O_4 , (b) Fe_3O_4 -chitosan and nanoparticle size histogram of (c) Fe_3O_4 , (d) Fe_3O_4 -chitosan

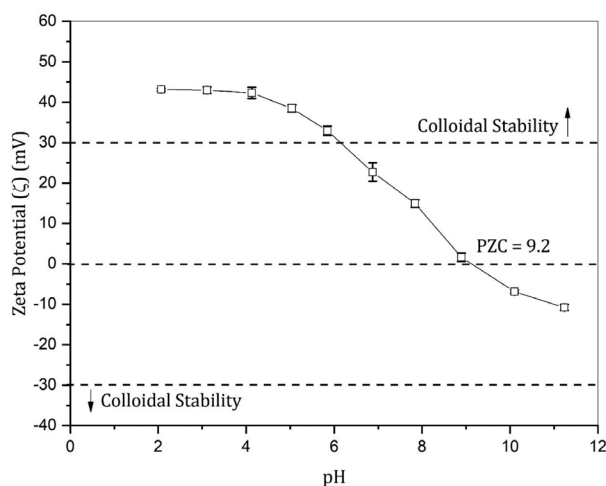


Figure 4. Zeta potential results from Fe₃O₄-chitosan nanoparticles

effluent containing various metal ions. They showed that the adsorbents were promising, and the adsorptive capacity of Fe₃O₄-chitosan nanoparticles was more efficient in removing metal ions than the bioadsorbent.

Based on these results, Fe₃O₄-chitosan nanoparticles were tested as metal adsorbents in the wastewater samples. Figure 5 shows the metal concentrations before and after adsorption and the percentage of metal removal. Among the metals analyzed in the study, the water sample showed the presence of aluminum, barium, iron, manganese and zinc ions. The metal ions lead, copper and chromium were not found. Aluminum and iron were above the legal limit for the standard release recommended by the Brazilian resolution for Class II rivers: 0.1 and 0.3 mg L⁻¹, respectively.^{6,7} The other metals were below the limit.

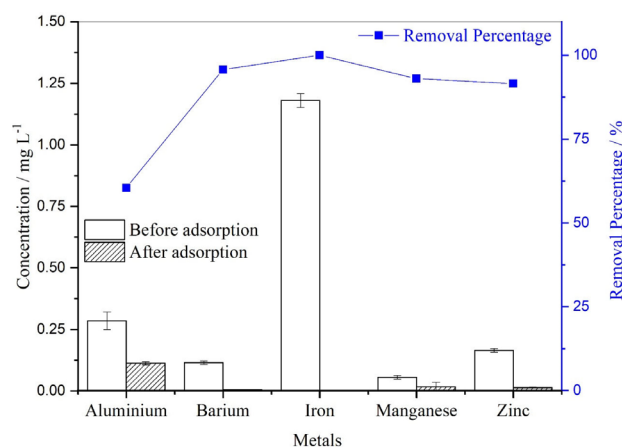


Figure 5. Concentrations and metal removal percentage before and after adsorption. The legal limits of aluminum, barium, iron, manganese, and zinc established by Brazilian laws⁷ are 0.1, 0.7, 0.3, 0.1, and 0.18 mg L⁻¹, respectively

Figure 5 shows that the metal removal percentage was more selective for Ba, Fe, Mn, and Zn (above 90%). For aluminum, the removal percentage was about 60%. Even when more than half of the aluminum was removed, the final concentration of this metal (0.108 mg L⁻¹) remained above

the limit allowed by Brazilian law, which is 0.100 mg L⁻¹. However, according to the World Health Organization (WHO), concentrations of less than 100-200 ppb of aluminum in water are acceptable.³²

This result is directly related to the zeta potential profile of Fe₃O₄ chitosan nanoparticles. The pH dependence can improve or worsen the metal adsorption on nanostructures, *i.e.* the pH of the solution is crucial for the adsorption of metal ions, because it directly influences the interactions between the adsorbent and the adsorbate.³³ The results showed that at pH values close to 7 (natural of the wastewater) it was possible to achieve a high efficiency in the simultaneous removal of metal ions present in the wastewater sample. This suggests a phenomenon of competition for the active site of the adsorbent between the metal ions and the protons (H⁺) present in the solution, as well as the formation of possible complexes between the metals, anions and water with electrically neutral charges, or even the tendency of the surface charges of the adsorbent to be protonated due to the increase of H⁺ in the solution.^{22,34,35} At pH values above 4 for the adsorbents containing chitosan, the adsorption tends to increase with increasing pH, and this phenomenon can be explained by the possible formation of hydroxy-complex species of the [(Metal).(OH)]⁺ species in the solution, which favors adsorption at pH values above the surface of the adsorbent, which is composed of polar groups (hydroxyl, carboxyl, amine, etc.), possibly negatively charged.^{22,34,35} In addition, the formation of other complexes such as [(Metal).(OH)²] confers neutrality and stability to the system, favoring equilibrium between the species and the surface of the adsorbent. The distribution of aluminum, iron and zinc species as a function of pH variation is described below.

For instance, the predominant species of aluminum in acidic conditions and at a pH below 5 is the Al³⁺ ion.³⁶ As acidity decreases, the species undergoes deprotonation in the [Al(OH)]²⁺ and [Al(OH)₂]⁺ structures, the Al(OH)₃ species prevails near a pH of 7, and the Al(OH)₄⁻ species dominates with increased basicity.³⁶ For instance, the predominant species of iron in acidic conditions and a pH below 3 is the Fe³⁺ ion.³⁷ When acidity decreases, the species experiences deprotonation in the [Fe(OH)₂]⁺ structures is dominant in the interval of pH 3 to 6, the Fe(OH)₃ species dominant in the pH between 6 to 10, and the Fe(OH)₄⁻ species dominates with increased above pH 10. The Fe(II) species dominate below pH 8.5.³⁷ The distribution of the species for zinc, at pH below 7.8 the Zn²⁺ species is dominant. Among the pH of 7.8 to 9 the dominant species is Zn(OH)⁺. The dominant species Zn(OH)₂/ZnO is in the pH range of 9 to 11.5. Between pH 11.5 and 12.5 there is a predominance of the species Zn(OH)₃⁻ and above pH 12.5 the species Zn(OH)₄²⁻ are dominant.³⁸ Thus, at pH 7.0 and according to the distribution of the aforementioned species, the states of aluminum, zinc and iron are in the forms: Al(OH)₃, Fe(OH)₃ and Fe²⁺ and Zn²⁺.

In real samples, aiming at large-scale *in situ* applications, pH adjustment in a water treatment plant or river may

represent an environmental concern. It is worth mentioning that nanoparticles are more positively charged for pH values between 2.0 and 6.0, which may increase the electrostatic repulsion between particles and heavy metals and interfere with this adsorption. The nanoparticles charge (obtained by zeta potential) becomes more positive when chitosan is added. Since the adsorption process was efficient, at the pH studied, it seems that the surface charge has little effect on the adsorption process, so it is possible that adsorption occurs due to the high chemical affinity of the studied metals with the nanostructured matrix. Chang *et al.*⁹ studied the adsorption of Cu²⁺ ions on Fe₃O₄@chitosan nanoparticles at pH 5 and obtained excellent results, which corroborates our results.

The percentage removal results indicate relatively fast metal adsorption on the active sites of Fe₃O₄-chitosan nanoparticles. In our study, the contact time was 60 minutes. Adsorption times reported in the literature range from 1 to 120 minutes.^{13,28-29}

Several studies have performed adsorption for simulated metal solutions, such as Cu(II)^{13,26,39}. In the present case, the percentage of metal removal was related to the chemical affinity with Fe₃O₄-chitosan nanoparticles (Fe > Ba > Mn > Zn > Al), considering that they have functional groups that can adsorb metal ions.

These results suggest that aluminum, barium, iron, manganese, and zinc interact with the amino group in chitosan, the same found by Wang *et al.*,¹⁰ who showed that an increase in adsorption capacity may be related to the complexation reaction of Cu(II), Co(II), Ni(II), Zn(II), Cr(VI), and Cd(II) by amino groups. Furthermore, this complexation results in complexes with removal efficiencies greater than 99%.²

The results also make sense in terms of nanoparticle properties. Chitosan improved colloidal stability and contributed to metal adsorption. Dotto *et al.*²⁷ showed that pure chitosan is a suitable adsorbent for dyes. The main advantage of coating Fe₃O₄ nanoparticles with chitosan is the improvement of their colloidal stability due to active functional groups interacting with the metal ions in the solution.² According to Keshvardoostchokami *et al.*,⁴⁰ chitosan-iron oxide nanocomposite adsorbents may be used to remove high metal ion concentrations from wastewater. Furthermore, the use of magnetic nanoparticles facilitates the separation of nanoparticles from the wastewater solution using an external magnetic field.⁴

4. Conclusions

In this study, Fe₃O₄ and Fe₃O₄-chitosan nanoparticles were synthesized, characterized, and used for metal removal from wastewater by adsorption. The synthesized nanoparticles exhibited sizes around 17 ± 7 nm as verified by TEM. FTIR and zeta potential confirmed the functionalization of Fe₃O₄ nanoparticle surfaces. In addition, at pH below 6.0, chitosan-

coated Fe₃O₄ nanoparticles exhibited higher surface charge (zeta potential), indicating improved colloidal stability. After adsorption in wastewater samples, the removal percentages of barium, iron, manganese and zinc were above 90% and about 60% for aluminum. FTIR analysis of the nano-adsorbent after adsorption indicated that the metals were bound to Fe₃O₄-chitosan nanoparticles. Our results are interesting because they show that Fe₃O₄-chitosan is highly capable of simultaneously removing metals in samples with a very complex matrix (wastewater) at room temperature, which shows the potential of this nanoparticles.

Acknowledgments

The authors would like to thank FAPESP (São Paulo Research Foundation) for the financial support (process number 2015/22864-2).

References

1. Segura, F. R.; Nunes, E. A.; Paniz, F. P.; Paulelli, A. C. C.; Rodrigues, G. B.; Braga, G. U. L.; Pedreira Filho, W. R.; Barbosa Jr., F.; Cerchiaro, G.; Silva, F. F.; Batista, B. L.; Potential risks of the residue from Samarco's mine dam burst (Bento Rodrigues, Brazil). *Environmental Pollution* **2018**, *218*, 813. [[Crossref](#)] [[PubMed](#)]
2. Bolisetty, S.; Peydayesh, M.; Mezzenga, R.; Sustainable technologies for water purification from heavy metals: review and analysis. *Chemical Society Reviews* **2019**, *48*, 463. [[Crossref](#)] [[PubMed](#)]
3. Abadian, S.; Rahbar-Kelishami, A.; Norouzbeigi R.; Peydayesh M.; Cu(II) adsorption onto *Platanus orientalis* leaf powder: Kinetic, isotherm, and thermodynamic studies. *Research on Chemical Intermediates* **2015**, *41*, 7669. [[Crossref](#)]
4. Akbarzadeh A.; Samiei M.; Davaran, S.; Magnetic nanoparticles: preparation, physical properties, and applications in biomedicine. *Nanoscale Research Letters* **2012**, *7*, 144. [[Crossref](#)] [[PubMed](#)]
5. Qu, X.; Alvarez, P. J. J.; Li, Q.; Applications of nanotechnology in water and wastewater treatment. *Water Research* **2013**, *47*, 3931. [[Crossref](#)] [[PubMed](#)]
6. CONAMA – Conselho Nacional do Meio Ambiente, Resolução n° 357. Dispõe sobre a classificação dos corpos de água e diretrizes ambientais para o seu enquadramento, bem como estabelece as condições e padrões de lançamento de efluentes, e dá outras providências, 2005. [[Link](#)]
7. CONAMA - Conselho Nacional do Meio Ambiente, Resolução n° 430. Dispõe sobre as condições e padrões de lançamento de efluentes, complementa e altera a Resolução no 357, de 17 de março de 2005, do Conselho Nacional do Meio Ambiente-CONAMA, 2011. [[Link](#)]
8. Hai, B.; Wu, J.; Chen, X.; Protasiewicz, J. D.; Scherson, D. A.; Metal-ion adsorption on carboxyl-bearing self-assembled monolayers covalently bound to magnetic nanoparticles. *Langmuir* **2005**, *21*, 3104. [[Crossref](#)] [[PubMed](#)]

9. Chang, Y.-C.; Chang, S.-W.; Chen, D.-H.; Magnetic chitosan nanoparticles: Studies on chitosan binding and adsorption of Co(II) ions. *Reactive and Functional Polymers* **2006**, *66*, 335. [[Crossref](#)]
10. Wang, J.; Zheng, S.; Shao, Y.; Liu, J.; Xu, Z.; Zhu, D.; Amino-functionalized Fe₃O₄@SiO₂ core-shell magnetic nanomaterial as a novel adsorbent for aqueous heavy metals removal. *Journal of Colloidal and Interface Science* **2010**, *349*, 293. [[Crossref](#)] [[PubMed](#)]
11. Tang, S. C. N.; Lo, I. M. C.; Magnetic nanoparticle: Essential factors for sustainable environmental applications. *Water Research* **2013**, *47*, 2613. [[Crossref](#)] [[PubMed](#)]
12. Cornell, R. M.; Schwertmann, U.; The iron oxides: Structure, Properties, Reactions, Occurrences and Uses. 2nd. ed., Wiley-VCH, Weinheim, New York, 2003.
13. Oliveira, L. C. A.; Fabris, J. D.; Pereira, M. C.; Óxidos de ferro e suas aplicações em processos catalíticos: Uma revisão. *Química Nova* **2013**, *36*, 123. [[Crossref](#)]
14. Pipi, A. R. F.; Magdalena, A. G.; Giafferis, G. P.; da Silva, G. H. R.; Piacenti-Silva, M.; Evaluation of metal removal efficiency and its influence in the physicochemical parameters at two sewage treatment plants. *Environmental Monitoring and Assessment* **2018**, *190*, 263. [[Crossref](#)] [[PubMed](#)].
15. CETESB (2013). Ficha de Informação Toxicológica. Divisão de Toxicologia, Genotoxicidade e Microbiologia Ambiental. [[Link](#)]
16. Gupta, A. K.; Gupta, M.; Synthesis and surface engineering of iron nanoparticles for biomedical applications. *Biomaterials* **2005**, *26*, 3995. [[Crossref](#)] [[PubMed](#)]
17. Bini, R.; Marques, R. F. C.; Santos, F. J.; Chaker, J. A.; Jafelicci Jr, M.; Synthesis and functionalization of magnetite nanoparticles with different amino-functional alkoxy silanes. *Journal of Magnetism and Magnetic Materials* **2012**, *324*, 534. [[Crossref](#)]
18. Laurent, S.; Forge, D.; Port, M.; Roch, A.; Robic, C.; Elst, L. V.; Muller, R. N.; Magnetic iron oxide nanoparticles: Synthesis, stabilization, Vectorization, physicochemical characterizations, and biological applications. *Chemical Reviews* **2008**, *108*, 2064. [[Crossref](#)] [[PubMed](#)]
19. Warner, C. L.; Addleman, R. S.; Cinson, A. D.; Droubay, T. C.; Engelhard, M. H.; Nash, M. A.; Yantasee, W.; Warner, M. G.; High-Performance, superparamagnetic, nanoparticle-based heavy metals sorbents for removal of contaminants from natural Waters. *ChemSusChem* **2010**, *3*, 749. [[Crossref](#)] [[PubMed](#)]
20. Yang, J.; Zeng, Q.; Peng, L.; Lei, M.; Song, H.; Tie, B.; Gu, J.; La-EDTA coated Fe₃O₄ nanomaterial: Preparation and application in removal of phosphate from water. *Journal of Environmental Sciences* **2013**, *25*, 413. [[Crossref](#)] [[PubMed](#)]
21. Magdalena, A. G.; Silva, I. M. B.; Marques, R. F. C.; Pipi, A. R. F.; Lisboa-Filho, P. N.; Jafelicci Jr. M.; EDTA-Functionalized Fe₃O₄ nanoparticles. *Journal of Physics and Chemistry of Solids* **2018**, *113*, 5. [[Crossref](#)]
22. Leandro-Silva, E.; Pipi, A. R. F.; Magdalena, A. G.; Piacenti-Silva, M.; Study of simultaneous adsorption efficiency of metals using modified organic and synthetic adsorbents. *Matéria* **2022**, *27*, e20220033. [[Crossref](#)]
23. Silveira, M. L. D. C.; Silva, I. M. B.; Magdalena, A. G.; Synthesis and characterization of Fe₃O₄-NH₂ and Fe₃O₄ - NH₂- chitosan nanoparticles. *Cerâmica* **2021**, *67*, 295. [[Crossref](#)]
24. APHA (2012) Standard Methods for the Examination of Water and Waste Water. 22nd Edition, American Public Health Association, American Water Works Association, Water Environment Federation. Washington, 2012.
25. Pancras, J. P., Norris, G. A.; Landis, M. S.; Kovalcik, K. D.; McGee, J. K.; Kamal, A. S.; Application of ICP-OES for evaluating energy extraction and production wastewater discharge impacts on surface waters in Western Pennsylvania. *Science of The Total Environment* **2015**, *529*, 21. [[Crossref](#)] [[PubMed](#)]
26. Leandro-Silva, E.; Pipi, A. R. F.; Magdalena, A. G.; Piacenti-Silva, M.; Application of Langmuir and Freundlich models in the study of banana peels bioadsorbent of copper (II) in aqueous medium. *Matéria* **2020**, *25*, e-12656. [[Crossref](#)]
27. Dotto, G. L.; Vieira, M. L. G.; Gonçalves, J. O.; Pinto, L. A. A.; Remoção dos Corantes azul brilhante, amarelo crepúsculo e amarelo tartrazina de soluções aquosas utilizando carvão ativado, terra ativada, terra diatomácea, quitina e quitosana: estudos de equilíbrio e termodinâmica. *Química Nova* **2011**, *34*, 1193. [[Crossref](#)]
28. Cullity, B. D.; Elements of X-Ray Diffraction. 2nd ed., London, 1977, p. 411. [[Crossref](#)]
29. Neves, R. P.; Bronze-Uhler, E. S.; Santos, P. L.; Lisboa-Filho, P. N.; Magdalena, A. G.; Salicylic acid incorporation in Fe₃O₄-BSA nanoparticles for drug release. *Química Nova*, 2021, *44*, 824. [[Crossref](#)]
30. Arias, J. L.; Reddy, L. H.; Couvreur, P.; Fe₃O₄/chitosan nanocomposite for magnetic drug targeting to cancer. *Journal of Materials Chemistry* **2012**, *22*, 7622. [[Crossref](#)]
31. Canela, K. M. N. C.; Garcia, R. B.; Caracterização de quitosana por cromatografia de permeação em gel - Influência do método de preparação e do solvente. *Química Nova* **2001**, *24*, 13. [[Crossref](#)]
32. Guidelines for Drinking-Water Quality; 4th edition, World Health Organization (WHO), **2017**, *4*, 222. [[Link](#)]
33. Hossain, M. A.; Ngo, H.H.; Guo, W.S., Nguyen, T. V.; Removal of copper from water by adsorption onto banana peel as bioadsorbent, *International Journal of GEOMATE*, **2012**, *2227*. [[Crossref](#)]
34. Nascimento, R. F.; Souza Neto, V. O.; Melo, D. Q.; Uso de Bioadsorbentes Lignocelulósicos na Remoção de Poluentes de Efluentes Aquosos. 1ª ed., Fortaleza, Imprensa Universitária, **2014**. [[Link](#)]
35. Bautista-Toledo, I.; Ferro-Garcia, M. A.; Rivera-Utrilla, J.; Moreno-Castilla, C.; Fernández, F. J. V.; Bisphenol a removal from water by activated carbon. Effects of carbon characteristics and solution chemistry. *Environmental Science Technology*, **2005**, *39*, 6246. [[Crossref](#)]
36. Echart, C. L.; Cacalli-Molina, S.; Aluminum phytotoxicity: Effects, tolerance mechanisms and its genetic control. *Ciência Rural* **2001**, *31*, 531. [[Link](#)]
37. Ngobeni, P. V.; Basitere, M.; Thole, A.; Treatment of poultry slaughterhouse wastewater using electrocoagulation: a review. *Water Practice & Technology* **2022**, *17*, 38. [[Crossref](#)]

38. Heakal, F. E-T.; Abd-Ellatif, W. R.; Tantawy, N. S.; Taha, A. A.; Impact of pH and temperature on the electrochemical and semiconducting properties of zinc in alkaline buffer media. *RSC Advances* **2018**, *8*, 3816. [[Crossref](#)]
39. Gao, J.; He, Y.; Zhao, X.; Ran, X.; Wu, Y.; Su, Y.; Dai, J.; Single step synthesis of amine-functionalized mesoporous magnetite nanoparticles and their application for copper ions removal from aqueous solution. *Journal of Colloid Interface Science* **2016**, *481*, 220. [[Crossref](#)] [[PubMed](#)]
40. Keshvardoostchokami, M.; Babaei, L.; Zamani, A. A.; Parizanganeh, A. H.; Piri, F.; Synthesized chitosan/iron oxide nanocomposite and shrimp shell in removal of nickel, cadmium and lead from aqueous solution. *Global Journal of Environmental Science and Management* **2017**, *3*, 267. [[Crossref](#)]